Science of the Total Environment 625 (2018) 872–884

Contents lists available at ScienceDirect

Science of the Total Environment

journal homepage: www.elsevier.com/locate/scitotenv

Internal phosphorus loading from sediments causes seasonal nitrogen limitation for harmful algal blooms

Shiming Ding [a,*], Musong Chen [a], Mengdan Gong [a], Xianfang Fan [a], Boqiang Qin [a], Hai Xu [a], ShuaiShuai Gao [a,b], Zengfeng Jin [a,b], Daniel C.W. Tsang [c], Chaosheng Zhang [d]

[a] State Key Laboratory of Lake Science and Environment, Nanjing Institute of Geography and Limnology, Chinese Academy of Sciences, Nanjing 210008, China
[b] University of Chinese Academy of Sciences, Beijing 100049, China
[c] Department of Civil and Environmental Engineering, The Hong Kong Polytechnic University, Hung Hom, Kowloon, China
[d] GIS Centre, Ryan Institute and School of Geography and Archaeology, National University of Ireland, Galway, Ireland

HIGHLIGHTS

- High-resolution sampling showed seasonal variations in distribution of mobile P in sediments.
- SRP diffusion flux at the sediment-water interface varied from −0.01 to 6.76 mg/m^2/d.
- Spatial-temporal variation in mobile P was controlled by microbe-mediated Fe redox cycling.
- Internal P loading accounted for 54% of increased water column TP during the prebloom-bloom period.
- Internal P loading played a major role in causing seasonal nitrogen limitation for HABs.

GRAPHICAL ABSTRACT

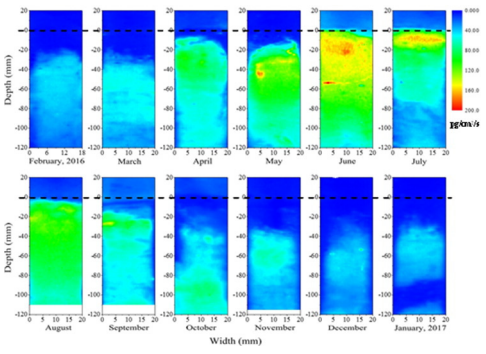

ARTICLE INFO

Article history:
Received 4 November 2017
Received in revised form 31 December 2017
Accepted 31 December 2017
Available online 4 January 2018

Editor: F.M. Tack

Keywords:
Lake sediment
Mobile phosphorus
Eutrophication
High-resolution sampling
Iron redox cycle
Harmful algal blooms

ABSTRACT

It is proposed that the internal loading of phosphorus (P) from sediments plays an important role in seasonal nitrogen (N) limitation for harmful algal blooms (HABs), although there is a lack of experimental evidence. In this study, an eutrophic bay from the large and shallow Lake Taihu was studied for investigating the contribution of internal P to N limitation over one-year field sampling (February 2016 to January 2017). A prebloom-bloom period was identified from February to August according to the increase in Chl*a* concentration in the water column, during which the ratio of total N to total P (TN/TP) exponentially decreased with month from 43.4 to 7.4. High-resolution dialysis (HR-Peeper) and diffusive gradients in thin films (DGT) analysis showed large variations in the vertical distribution of mobile P (SRP and DGT-labile P) in sediments, resulting in the SRP diffusion flux at the sediment-water interface ranging from −0.01 to 6.76 mg/m^2/d (minus sign denotes downward flux). Significant and linear correlations existed between SRP and soluble Fe(II) concentrations in pore water, reflecting that the spatial-temporal variation in mobile P was controlled by microbe-mediated Fe redox cycling. Mass estimation showed that the cumulative flux of SRP from sediments accounted for 54% of the increase in TP observed in the water column during the prebloom-bloom period. These findings are supported by the significantly negative correlation ($p < 0.01$) observed between sediment SRP flux and water column TN/TP during the same period. Overall, these results provide solid evidence for the major role of internal P loading in causing N limitation during the prebloom-bloom period.

* Corresponding author.
E-mail address: smding@niglas.ac.cn (S. Ding).

https://doi.org/10.1016/j.scitotenv.2017.12.348
0048-9697/

1. Introduction

Harmful algal blooms (HABs) are occurring worldwide with increasing magnitude and frequency. They seriously threaten the balance of lake ecosystems, posing a risk to public health by affecting drinking water supplies, food security, and recreational use (Brooks et al. 2016). HABs are an established indicator of water eutrophication, which is caused by the over-enrichment of anthropogenic nutrients in water bodies (Paerl and Otten 2013). Nitrogen (N) and phosphorus (P) are key nutrients in eutrophication; they play a dominant role in the promotion of HABs with significantly increased concentrations in freshwater ecosystems (Peñuelas et al. 2013; Schindler et al. 2016; Tong et al. 2017).

During previous decades, P was regarded as the prime limiting nutrient in freshwater ecosystems (Schelske 2009; Schindler et al. 2008, 2016), based on the evidence from multiscale experiments including long-term case studies and multi-year whole lake assessments (Ho and Michalak 2017; Schindler et al. 2008, 2016). Accordingly, P limitation has received more research attention than N limitation, encouraging the development of effective control measures for P input, while the control of N is assumed to be offset by cyanobacterial N_2 fixation (Correll 1998; Lewis et al. 2011; Schindler et al. 2008). However, the results of nutrient enrichment experiments at a range of scales, from bottle bioassay to whole lake, have shown that the mass growth of phytoplankton and the formation of HABs are controlled by enrichment of both N and P, rather than N or P alone (Chen et al. 2013; Lewis and Wurtsbaugh 2008; Lewis et al. 2011; Paerl et al. 2016; Xu et al. 2015). The limiting roles of N and P have been found to vary temporally across seasons, geographically with regions, and even spatially within a lake. P limitation is commonly observed in spring, whereas it often changes to N limitation in summer and fall, when temperature and meteorological conditions favor the formation of HABs (Bullerjahn et al. 2016; Chaffin et al. 2013; Janssen et al. 2017). The change in paradigm from P limitation to dual limitation is because cyanobacterial N_2 fixation cannot always fulfil the N requirement by lake ecosystems. Inputs of P can be sustained by the release of P from sediments, while N deficits often occur due to denitrification (Lewis et al. 2011; Paerl et al. 2016).

The release of P due to internal sediment loading has been well recognized (Janssen et al. 2017; Lepori and Roberts 2017; Paytan et al. 2017; Xie et al. 2003), with P release persisting for typically 5–15 years after the reduction of external P inputs (Jeppesen et al. 2005; Watson et al. 2016; Welch and Cooke 2005). The rate of sediment P release can vary seasonally, with increases normally observed in warm seasons (Spears et al. 2012; Yang et al. 2013). It has been reported that in some lakes the contribution of sediment P release into the water column exceeds the external P input and becomes a critical factor influencing HABs (Nürnberg and LaZerte 2016; Penn et al. 2000; Sondergaard et al. 2003; Wu et al. 2017). In some cases, internal diffusive recycling of P cannot trigger HABs on its own, but can cause blooms when combined with increased external P loads (Matisoff et al. 2016). However, there are few experimental evidences to prove the theory that internal P loading from sediments can induce imbalance in N and P concentrations, and that the seasonal variation changes from P limitation to N limitation (Orihel et al. 2015).

In this study, a semi-enclosed bay in Lake Taihu was selected to study the effect of internal P loading on seasonal nutrient limitation in the water column. High-resolution dialysis (HR-Peeper) and diffusive gradients in thin films (DGT) samplers were used to measure the distributions of mobile P and Fe(II) in sediments. The diffusion flux across the sediment-water interface (SWI) was calculated along with its contribution to the water column P, allowing the role of internal P loading on the formation of seasonal N limitation to be assessed.

2. Materials and methods

2.1. Lake description and field site

Lake Taihu is located in the southeastern region of the Yangtze River delta, in China's coastal plain (Fig. 1). It is a large and shallow lake, with a mean depth of around 2.0 m, covering a 2340 km^2 area. Harmful algal blooms were first reported in a few regions of Lake Taihu in the 1960s (Qin et al. 2004). The impacted regions gradually expanded to most of the lake by the mid- to late 1990s (Xu et al. 2017). During HAB events, cyanobacteria have been found to account for the majority of phytoplankton biomass (60–90%), based on Chl*a* concentrations (Otten et al. 2012; Xu et al. 2017). In May 2007, a highly publicized drinking water crisis occurred, in which the Wuxi city drinking water plant ceased functioning due to a very large "cyanobacteria mat" (Qin et al. 2010). Following this, a wide range of measures were implemented by Chinese central and local government to reduce external nutrient loading to the lake (Wu and Hu, 2008; Yang and Liu 2010). As a result, the concentrations of TN and TP in Meiliang Bay consistently decreased after 2007, returning to the level observed in the early of 1990s (Xu et al. 2017). However, Chl*a* concentrations did not respond with the reductions of TN and TP as anticipated.

The sampling site is located in Meiliang Bay nearby the Taihu Laboratory for Lake Ecosystem Research (TLLER) (31°26′18″ N, 120°11′12″ E), Nanjing Institute of Geography and Limnology (Fig. 1). Meiliang Bay is one of the most eutrophic regions of Lake Taihu (Xu et al. 2014). The annual Chl*a* concentration in Meiliang Bay continued to increase to a peak of 43 μg/L from 2007 to 2009, remaining over 20 μg/L following this (Xu et al. 2017). The three rivers connecting to Meiliang Bay, Wujing Gang, Zhihu Gang and Liangxi River, have all been closed off by local government in order to prevent new input of external sewage into the bay.

2.2. Principles and preparation of HR-peeper and DGT samplers

The HR-Peeper device contained 30 equally spaced 200 μL chambers fully loaded with deionized water, with a 4.0 mm vertical resolution (Ding et al. 2010; Xu et al. 2012) and the chamber surfaces were covered using a 0.45 μm cellulose nitrate membrane. The concentration of soluble analytes present in sediment pore water, was measured by analyzing sample solutions in chambers after equilibration.

DGT is a passive sampling technique for the measurement of the labile fraction of analytes (Zhang et al. 2014; Zhang and Davison 1995). Concurrently, high-resolution DGT measurements were performed at

Fig. 1. Location of the sampling site in Meiliang Bay of Lake Taihu (modified from Xu et al. 2017).

the two-dimensional level (2D), allowing a sensitive reflection of the localized changes of solution concentration and solid phase resupply (Ding et al. 2015; Santner et al. 2015). For this, a thin diffusion layer of 10 to 100 μm thickness is used, with DGT measurements typically interpreted as the time-averaged flux (μg cm^{-2} s^{-1}) (Santner et al. 2015) as shown in Eq. (1):

$$F_{DGT} = \frac{M}{At} \quad (1)$$

where t is the deployment time (s); A is the exposure area of the gel (cm^2); and M is the corresponding accumulated mass over the full deployment time (μg).

Zr-oxide DGT was used to measure labile P at a 2D-, submillimeter level (Ding et al. 2013), using molybdenum blue surface staining of the Zr-oxide binding gel (Ding et al. 2011). In the assembly of DGT probes, the Zr-oxide binding gel was covered with a Durapore® PVDF membrane (Millipore; 0.45 μm pore size; 0.10 mm thickness), assembled together using a new flat-type plastic holder (Ding et al. 2016b). Both Zr-oxide DGT and HR-Peeper probes were provided by EasySensor Ltd. (www.easysensor.net). They were deoxygenated with nitrogen for a minimum of 16 h prior to deployment.

2.3. Sampling and analysis

Nine sediment cores (9 cm in diameter, 30 cm in length) were collected each month from the sampling site, from February 2016 to January 2017. The thicknesses of the sediment and overlying water in each core were adjusted on site to about 20 cm. The cores were transported to the laboratory within 3 h post-collection. Three cores were put into a tank and incubated for 2–3 days to deploy the HR-Peeper and Zr-oxide DGT probes. The temperature was kept at the same level in the field using a circulating water bath. For deployment of HR-Peeper and Zr-oxide DGT probes, one HR-Peeper probe was first inserted into one of the cores and deployed for 24 h. Following this, a Zr-oxide DGT probe was then inserted into the same core and they were both incubated for a further 24 h. A preliminary test using cores collected in July, showed that in sediments the concentrations of dissolved oxygen (DO) and the DO penetration depth (OPD) did not change significantly pre- or post-incubation for 3 days (Fig. S1).

Three cores were used for the measurement of dissolved oxygen (DO) concentrations and redox state (Eh) in the water-sediment profiles, using oxygen and redox microelectrodes (Unisense, Denmark). The remaining three sediment cores were sliced into 1.0 cm sections down to a depth of 10 cm below the surface, under a N_2 atmosphere. The sediment segments were lyophilized at −80 °C and then stored at 4 °C for analysis. The sediment layer at depths of −20 to −30 mm (the minus denotes the depth below the SWI) was selected for analysis of bacterial abundance. The details of sample analyses are shown in Supporting Information.

2.4. Calculations of SRP flux across the SWI

The diffusion flux of SRP (F) across the SWI was calculated based on Fick' First Law (Boudreau 1996), according to Eq. (2) and the degree of sediment tortuosity (Boudreau 1996) was calculated using Eq. (3):

$$F = -\frac{\varphi D_0}{\theta^2}\frac{\partial C}{\partial z} \quad (2)$$

$$\theta^2 = 1 - \ln(\varphi^2) \quad (3)$$

where φ represents the sediment porosity (dimensionless); θ represents the sediment tortuosity (dimensionless); D_0 refers to the solute diffusion coefficient for $H_2PO_4^-$, C is the concentration of SRP (mg/L) determined using HR-Peeper; z represents the depth (mm); $\left(\frac{\partial C}{\partial z}\right)_{z=0}$ refers to the SRP concentration gradient (slope) in the vicinity of the SWI in concentration vs. depth data (typically 20 mm or less).

2.5. Statistical analyses

Statistical analysis was performed using SPSS v19.0 software. The correlations between each two variables were individually analyzed using the Pearson correlation coefficient, at the $p < 0.05$ and $p < 0.01$ levels of significance. The water quality data between February 2015 and January 2016 were also applied to the analysis, with monitoring data supplied by the TLLER.

3. Results

3.1. General water and sediment quality

Basic water quality characteristics are outlined in Table 1. Water temperatures varied from 9.2 to 31.2 °C, the concentration of DO varied from 5.95 to 12.2 mg/L, with the lowest levels appearing in July (5.95 mg/L) and August (6.32 mg/L). The pH values varied from 8.29 to 9.57, with the greatest values appearing in July (9.25) and then June (8.21). The concentration of Chl*a* ranged from 12.3 mg/L in February to 178.4 mg/L in October 2016, with the value in August also being relatively high (153.4 mg/L). The concentration of TN ranged from 1.63 mg/L in September to 4.92 mg/L in August, while the concentration of TP showed an increasing trend from 0.056 mg/L in February to 0.46 mg/L in August, followed by a reduction to 0.08 mg/L in January 2017. The ratio of TN to TP (TN/TP) showed a decreasing trend from 43.4 in February 2016 to 7.4 in September 2016, followed by an increasing trend to 21.2 in January 2017. A similar trend appeared with concentrations of Chl*a*, TN, TP, and TN/TP ratio from February 2015 to January 2016. In the two data sets, the concentrations of Chl*a* were positively correlated with TP concentrations (both $p < 0.01$), while no correlation existed between Chl*a* and TN concentrations.

The basic sediment quality characteristics are listed in Table 2. In the surface sediment layer, the concentrations of TOC, TN and TP showed slight variations. The concentrations of reactive Fe and P showed similar distributions at most of the sampling times, with extremely low values observed from April to May for Fe and from April to June for P (Fig. 2). The concentrations of bacterial abundance ranged from 1.33E + 11 to 11.4E + 11 copies, with the value in March being significantly greater than in all other months. The OPD ranged from 0.6 mm in June to 3.4 mm in February, with relatively low values (0.6 to 1.6 mm) apparent from June to August (Fig. 3). The Eh values decreased with sediment depth (Fig. 4), and all the mean values in the surface 3.5 cm layer were >300 mv (Table 2).

3.2. High-resolution distributions of soluble Fe(II) and SRP

The distributions of soluble Fe(II) and SRP in overlying water and pore water profiles are shown in Fig. 5. The concentrations of soluble Fe(II) and SRP showed a drastic increase from March to April, remaining high until July and August, followed by a decreasing trend afterwards. For all sampling times, both soluble Fe(II) and SRP showed similar changes with respect to increasing depth, i.e., presenting with an initially low and stable concentration distribution in the upper profile zones, followed by an increase in concentration to specific depths and then a decrease in concentration towards the bottom of the profile. In all samples, Fe and P showed a positive correlation to a very significant level ($p < 0.01$) (Fig. 5).

In order to better describe the characteristics of the SRP and soluble Fe(II) profiles, the depth of the onset of the increasing phase (D_{ip}), the maximum concentration in each profile (C_{max}), and the depth appearing the maximum concentration (D_{max}) are summarized in Table 3. For SRP, the D_{ip} became shallower from −20 mm in March to 4 mm from June to August, followed by a reduction to deeper levels of

Table 1
Water quality characteristics at the sampling site in Meiliang Bay, Lake Taihu, from February 2015 to January 2017.

Month	Feb 2016 to Jan 2017							Feb 2015 to Jan 2016[a]			
	T	DO	pH	Chla	TN	TP	TN/TP	Chla	TN	TP	TN/TP
	(°C)	(mg/L)		(μg/L)	(mg/L)	(mg/L)		(μg/L)	(mg/L)	(mg/L)	
Feb	9.2	12.21	8.31	12.3	2.43	0.056	43.4	13.2	2.35	0.057	41.3
Mar	10.5	10.05	8.36	21.4	2.95	0.078	37.8	21.5	2.93	0.073	40.2
Arp	20.0	10.02	8.68	16.7	3.52	0.102	34.5	19.9	3.97	0.117	33.9
May	19.8	8.41	8.29	12.5	1.97	0.068	28.9	25.9	2.48	0.083	29.9
Jun	26.1	8.21	9.57	64.3	1.69	0.112	15.4	55.1	2.28	0.105	21.7
Jul	29.0	5.95	9.25	112.3	3.34	0.233	14.5	69.5	1.66	0.097	17.1
Aug	31.2	6.32	8.54	153.4	4.92	0.462	10.7	121.6	2.24	0.237	9.5
Sep	24.8	7.21	8.39	38.9	1.63	0.221	7.4	46.3	1.79	0.267	6.7
Oct	19.7	8.66	8.73	53.4	2.88	0.354	8.2	174.8	4.39	0.414	10.6
Nov	16.1	9.67	8.52	178.4	2.52	0.272	9.3	87.0	1.89	0.161	11.8
Dec	9.5	11.28	8.43	35.5	2.17	0.123	17.6	21.4	1.16	0.067	17.3
Jan	7.5	10.4	8.34	14.4	1.65	0.078	21.2	12.5	1.43	0.065	22.0

[a] Monitored by Taihu Laboratory for Lake Ecosystem Research (TLLER).

−28 mm in December. The D_{max} also became shallower from −72 mm in March to −12 mm in July, followed by a lowering of depth to −84 mm in January 2017. The C_{max} increased from 0.133 mg/L in February to 1.73 mg/L in June, followed by a decrease to 0.01 mg/L in January 2017. The changes in D_{ip}, D_{max} and C_{max} for soluble Fe(II) were similar to those observed for SRP, with the shallowest D_{ip} being 4 mm between June and August, the shallowest D_{max} being −16 mm in September, and the maximum C_{max} being 5.31 mg/L in June.

3.3. Two-dimensional distributions of DGT-labile P

The 2D distributions of DGT-labile P (represented as DGT flux) for each month had imaging performed at the submillimeter level (Fig. 6). It is apparent that the DGT fluxes were relatively low throughout the full profile in February, but then they exhibited an increasing trend until June, followed by a decreasing trend until January 2017. The DGT fluxes were greatest in June, followed by July. Meanwhile, the maximum concentrations in June and July were higher than those in other months, with depths showing the maximum concentrations being closer to the SWI.

3.4. Diffusion fluxes of SRP across the sediment-water interface

The flux of SRP across the SWI for each month is presented in Fig. 7, ranging from −0.01 mg/m^2/d in December to 6.76 mg/m^2/d in June (minus sign denotes downward flux). The flux exhibited an increasing trend from February to July and remained at a high level until August (4.75–6.76 mg/m^2/d), followed by a decrease until December 2016. The maximum positive flux was observed in June and it was 337-fold higher than the minimum positive value in October. The SRP flux was found to be linearly correlated with OPD, temperature, and the three profile-feature parameters for mobile P (D_{ip}, D_{max} and C_{max}) (Fig. 8).

Table 2
Sediment characteristics at the sampling site in Meiliang Bay, Lake Taihu, from Feb 2016 to Jan 2017.

Month	TOC[a]	TN[a]	TP[a]	Reactive Fe[a]	Reactive P[a]	Eh[b]	OPD[c]	Bacterial abundance[d]
	(%)	(g/kg)	(g/kg)	(g/kg)	(mg/kg)	(mV)	(mm)	(Copies/g)
Feb	4.49	0.76	0.53	1.60	34.4	369.5	3.4	2.79E + 11
Mar	4.14	0.77	0.49	1.44	38.7	394.3	3.6	11.4E + 11
Arp	4.98	0.90	0.52	1.09	2.63	367.9	3.0	2.49E + 11
May	4.69	0.79	0.53	0.94	6.36	372.6	2.2	1.33E + 11
Jun	4.70	0.96	0.50	1.54	6.78	327.2	0.6	2.78E + 11
Jul	4.32	0.90	0.50	1.46	65.6	299.7	1.0	4.63E + 11
Aug	4.04	0.85	0.50	1.52	42.4	324.4	1.6	3.89E + 11
Sep	4,21	0.91	0.53	1.78	62.3	371.5	2.0	2.43E + 11
Oct	4.24	0.92	0.59	1.99	74.0	369.8	2.2	6.25E + 11
Nov	4.32	0.85	0.53	1.25	31.5	314.9	2.2	5.12E + 11
Dec	4.41	0.86	0.48	1.26	45.6	322.6	2.6	6.76E + 11
Jan	4.38	0.92	0.47	1.48	29.4	347.6	3.0	4.37E + 11

[a] Mean value in the surface 5 cm depth sediment layer.
[b] Mean value in the surface 3.5 cm depth sediment layer.
[c] Oxygen penetration depth.
[d] Mean value in the 20–30 mm depth sediment layer.

4. Discussion

4.1. Response of HABs to monthly changes in nutrients

Chl*a* concentrations exceeding 20 and 40 μg/L have been defined as blooms, in particular as harmful blooms in Lake Taihu (Xu et al. 2015). In this study, the monthly mean Chl*a* was 56 μg/L, reflecting that HABs in Meiliang Bay posed a very serious hazard (Table 1). The concentration of Chl*a* remained at low levels from February to May, with only the value in March exceeding 20 μg/L, allowing this period to be regarded as the prebloom phase. Chl*a* concentrations drastically increased from June to August with an extremely high concentration range (45–153 μg/L), i.e., identified as the bloom phase. This period is followed by a sharp decrease in Chl*a* concentration in September and then a rapid increase in November. This phenomenon has been observed in Taihu and other lakes (Giles et al. 2016), suggesting the occurrence of a bloom collapse in September and then the development of a late season bloom in November.

A significantly positive correlation was observed between Chl*a* and TP ($p < 0.01$), while no such correlation existed between Chl*a* and TN. This finding agrees with a statistical study performed by Xu et al., (2017), in which the annual mean TP concentration was significantly correlated to Chl*a* concentrations in Lake Taihu according to data covering the 1992–2012 period. Conversely, TN concentrations had weak or insignificant correlations with Chl*a* in the periods of 1992–2006 and 2007–2012, respectively. In combination with the study of Xu et al., (2017), this study evidences that phytoplankton biomass has a strong response to the change in TP concentrations, on both annual and monthly scales.

The concentrations of TP were low in winter (December and February in 2016 and January in 2017) and spring (March to May in 2016), while high concentrations were observed in summer (June to August in 2016) and fall (September to November in 2016). An inverse pattern was observed for TN concentrations in the water column, resulting in low TN/TP values in the summer and fall (7.4–15.4) compared to those in winter and spring (17.6–43.4). The variation in TN/TP observed was mainly caused by the change in TP concentrations, as the monthly variation in TP was much greater than that of TN (Table 1).

The TN/TP ratio has often been used for predicting whether N or P is limiting the growth of phytoplankton (Smith 2006; Verburg et al. 2013),

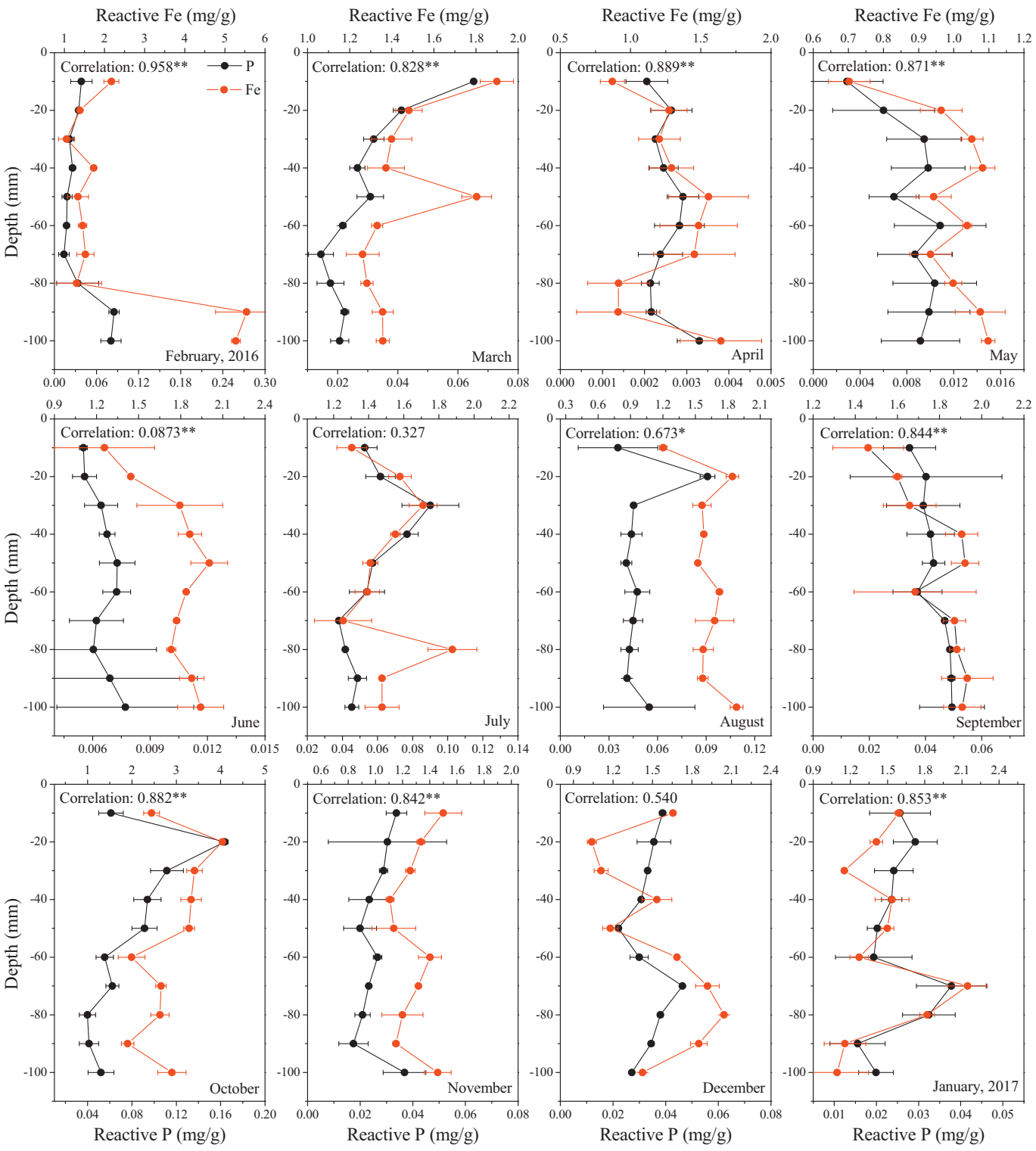

Fig. 2. Vertical distributions of reactive P and Fe concentrations in sediment cores, with 10 mm intervals sampled from Meiliang bay each month. Result indicate a correlation between reactive P and Fe concentrations, with significant correlations indicated by *for the 0.05 level and ** for the 0.01 level. Values are means ± SD of three replicate analyses.

based on the hypothesis that there is an optimal ratio of TN/TP that can promote maximum phytoplankton biomass production. Guildford and Hecky (2000) suggested that in both lakes and oceans, N limitation occurred at TN/TP < 9 whereas P limitation occurred when TN/TP > 22.6, and a TN/TP between 9 and 22 indicated N and P co-limitation. The TN/TP ratio threshold that causes the shift from P to N limitation varies in many field studies, partly due to the variation in phytoplankton species (Klausmeier et al. 2004). In Lake Taihu, the TN/TP ratio threshold used to identify N or P limitation was determined to be 21.5–24.7, at which nutrients were present below 7.75–13.95 mg/L TN and 0.41–0.74 mg/L TP (Ma et al. 2015). According to this criterion, P limitation occurred from February to May in 2016, while N limitation occurred from June in 2016 to January in 2017. This finding is in agreement with the results of dilution bioassay studies by Xu et al. (2015), showing that P limitation controlled the prebloom period and N limitation controlled the summer-fall bloom period.

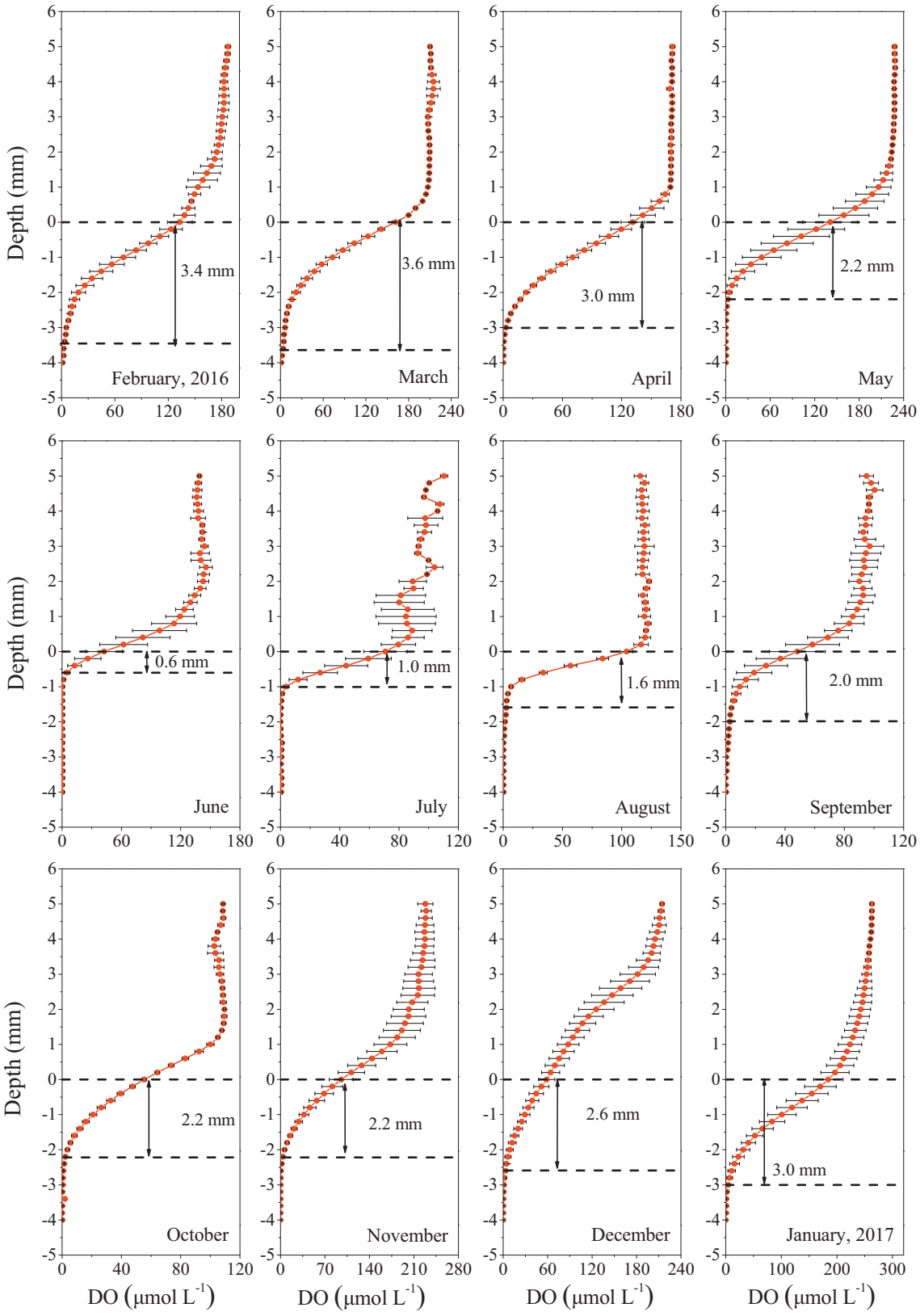

Fig. 3. Change in DO concentration and penetration depth in the sediment-water profiles for each month between Feb 2016 and Jan 2017. Values are means ±SD of three replicate analyses.

The indicative function of TN/TP was further supported by its relationship with Chl*a* concentrations during the prebloom-bloom phase. These relationships can be well fitted using an exponential equation covering the prebloom-bloom phases from February to August in 2015 and 2016 ($p < 0.01$) (Fig. 9A). No correlation could be revealed when the full annual dataset was analyzed (i.e., from January to December), demonstrating that the TN/TP ratio is more suitable for predicting nutrient limitation during the prebloom-bloom phases.

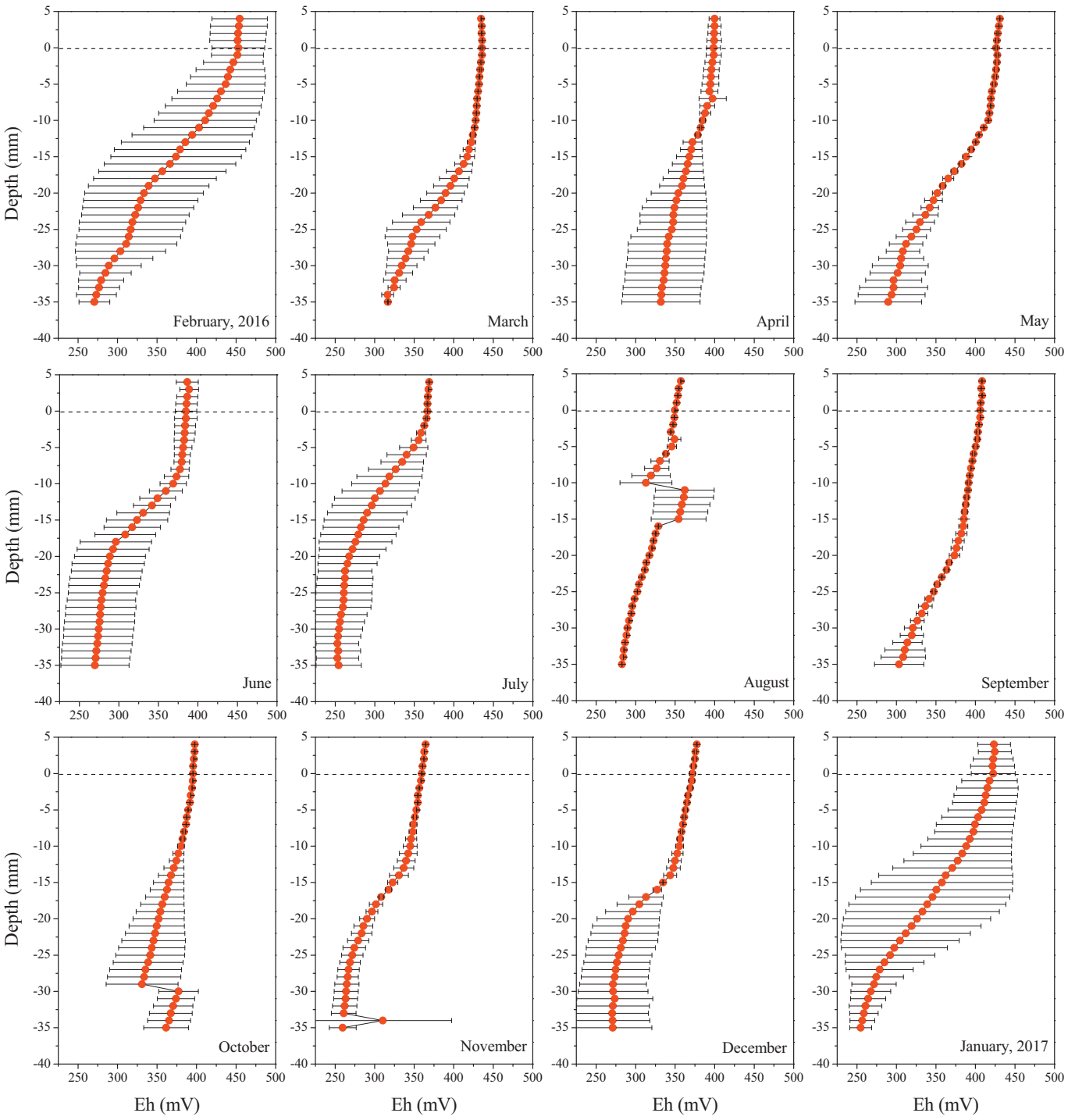

Fig. 4. Vertical change of Eh in the sediment-water profiles for each month between Feb 2016 and Jan 2017. Values are means ± SD of three replicate analyses.

4.2. Monthly changes in internal P loading and the controlling mechanisms

Pore water diffusive flux calculations showed a large variation in SRP flux across the SWI during sampling at Meiliang Bay (Fig. 7), with the release of P from sediments to overlying waters in all eleven months of the one-year sampling period. A high level of flux was observed at the SWI between April and September. The duration of internal P loading was found to be longer than reported in eutrophic Danish lakes, where sediments had a negative P retention from May to August (Søndergaard et al. 2013). The maximum flux (6.76 mg/m^2/d) appeared in June, with the lowest OPD (0.6 mm), reflecting that the upper sediment layer was nearly anoxic. It is of note that this value was much >1.9 mg/m^2/d, which was previously reported in Meiliang Bay using the static sediment incubation method (Zhang et al. 2006). In the static incubation experiment, the overlying water was pulled out and filtered through a 0.45 μm filter membrane to remove particle interference prior to static incubation; therefore, oxygen was inevitably introduced into the overlying water, causing the oxygenation of the upper sediment layer. This may be a contributing factor for the lower flux previously reported (Zhang et al. 2006).

The level of flux observed in this study was also greater than the values of 1.08 mg/m^2/d reported in Meiliang Bay (McCarthy et al.

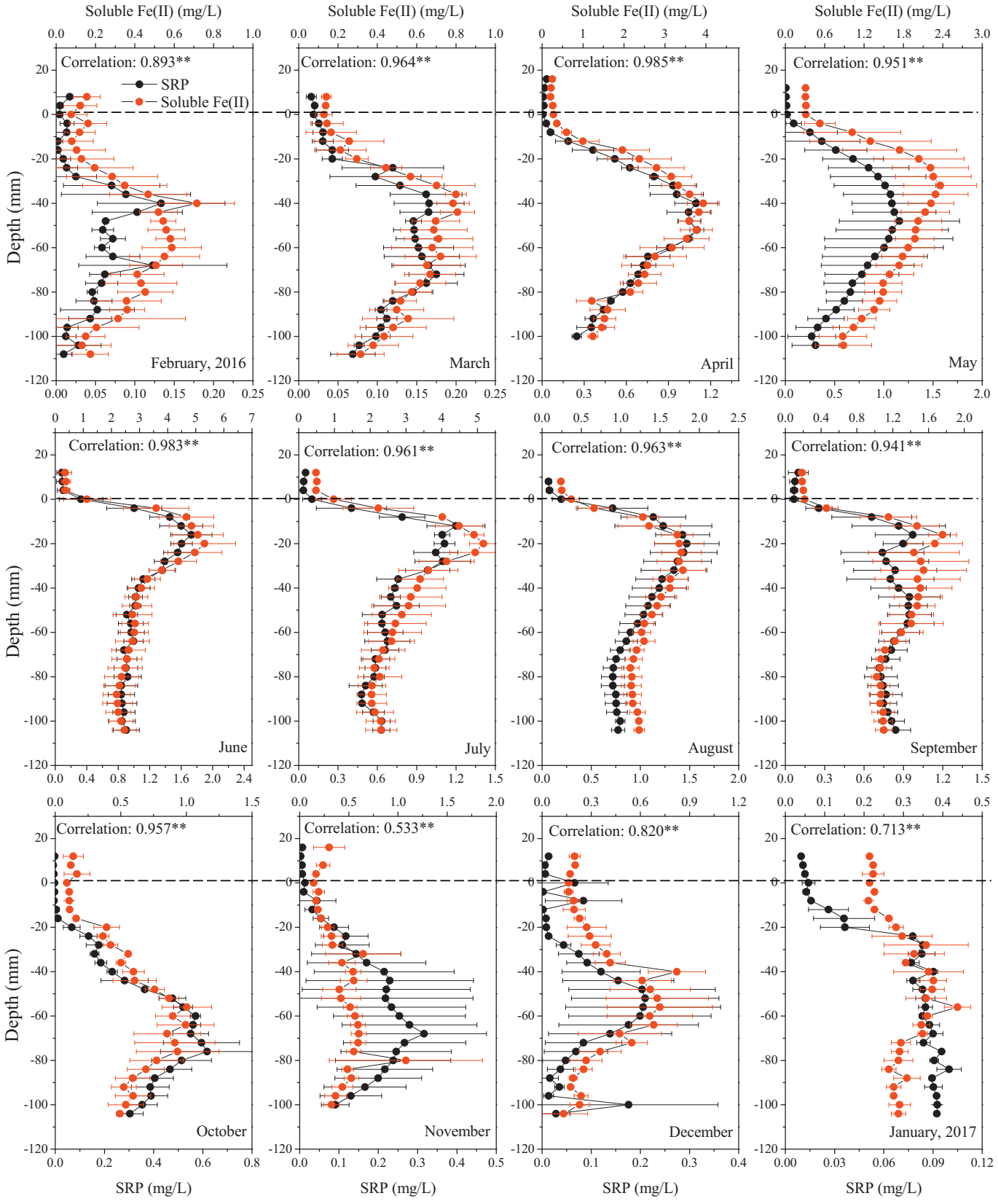

Fig. 5. Monthly distributions of soluble reactive P (SRP) and soluble Fe(II) in the sediment-water profiles of Meiliang Bay, Lake Taihu, from February 2016 to January 2017. Value shown is the correlation coefficient between SRP and soluble Fe(II), with double asterisks denoting significance to the $p < 0.01$ level.

2007), 0.16–2.91 mg/m^2/d reported in Lake Erie (Matisoff et al. 2016; Paytan et al. 2017), and 1.49 ± 1.8 mg/m^2/d reported in Lake Diefenbaker (Nürnberg et al. 2013) under aerobic incubation. On the other hand, the values in this study were lower than the previously reported values of 9.34 ± 6.48 mg/m^2/d (Matisoff et al. 2016) and 16.28 ± 3.48 mg/m^2/d (Doig et al. 2017) observed under anaerobic incubation

Table 3
Vertical distribution characteristics of the SRP and soluble Fe(II) profiles as shown in Fig. 5, in Meiliang Bay, Lake Taihu, from February 2016 to January 2017.

Month	SRP			Soluble Fe(II)		
	D_{ip}[a] (mm)	D_{max}[b] (mm)	C_{max}[c] mg/L	D_{ip} (mm)	D_{max} (mm)	C_{max} mg/L
Feb	−16	−40	0.133	−16	−40	0.817
Mar	−20	−72	0.175	−16	−44	0.807
Apr	−12	−40	1.097	−12	−40	3.936
May	0	−48	1.159	0	−32	2.363
Jun	4	−16	1.731	4	−20	5.311
Jul	4	−12	1.202	4	−20	5.167
Aug	4	−20	1.472	4	−24	1.772
Sep	0	−16	0.971	0	−16	1.756
Oct	−16	−76	0.618	−16	−76	0.933
Nov	−16	−68	0.316	−28	−68	0.601
Dec	−28	−56	0.213	−28	−44	0.823
Jan	−20	−84	0.012	−20	−56	0.437

[a] The depth showing onset of the increasing phase.
[b] Depth showing the maximum concentration in each profile.
[c] The maximum concentration in each profile.

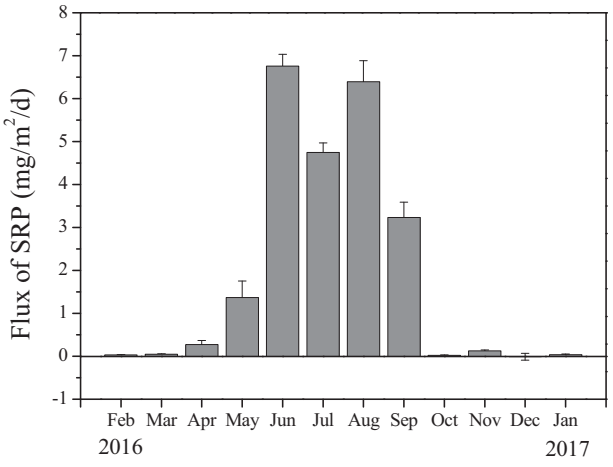

Fig. 7. Diffusion flux of SRP across the sediment-water interface, in Meiliang Bay, Lake Taihu, from February 2016 to January 2017.

in Lakes Erie and Diefenbaker. This further demonstrates that the magnitude of SRP flux at the SWI in Meiliang Bay are at an intermediate level between oxic and anoxic conditions.

The change in SRP flux across the SWI was a result of vertical changes to SRP concentrations in the sediment-water profile. The high SRP flux originated from a steep SRP concentration gradient at the SWI, coupled with a low D_{ip} and D_{max} as well as high C_{max} values (Table 3, Fig. 5). The greatest D_{max} value was observed in the region extending from the depths of −12 mm to −84 mm. This change in mobile P in sediments was even more evident with 2D imaging of DGT-labile P (Fig. 6). This reflects the high mobility of P in sediments, which induces high seasonal fluctuation, with the reactive sediment layer displaying a

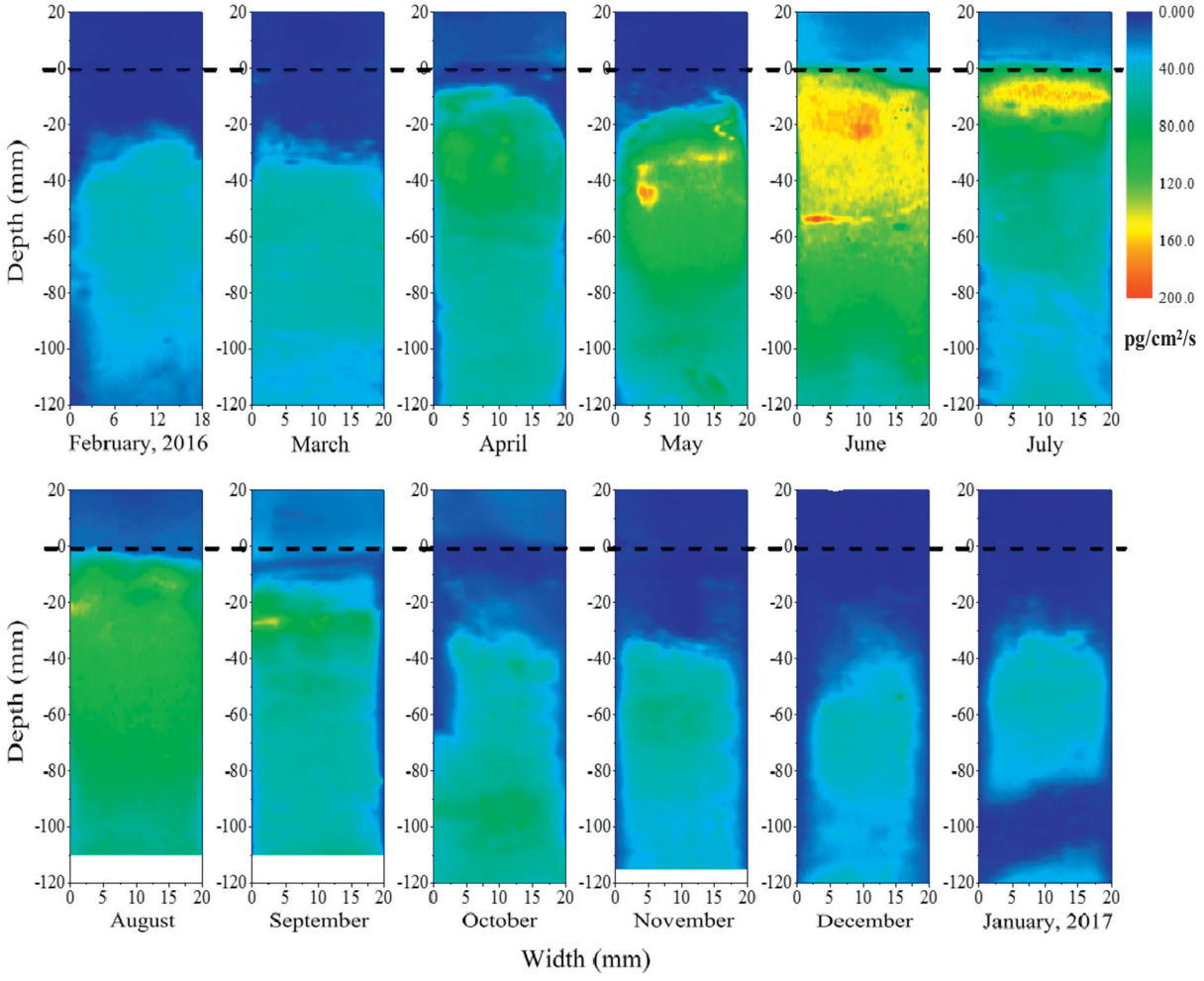

Fig. 6. Two-dimensional heat-map distributions of labile P concentrations in the sediment-water profiles as measured by DGT probe analysis, in Meiliang Bay, Lake Taihu, from February 2016 to January 2017.

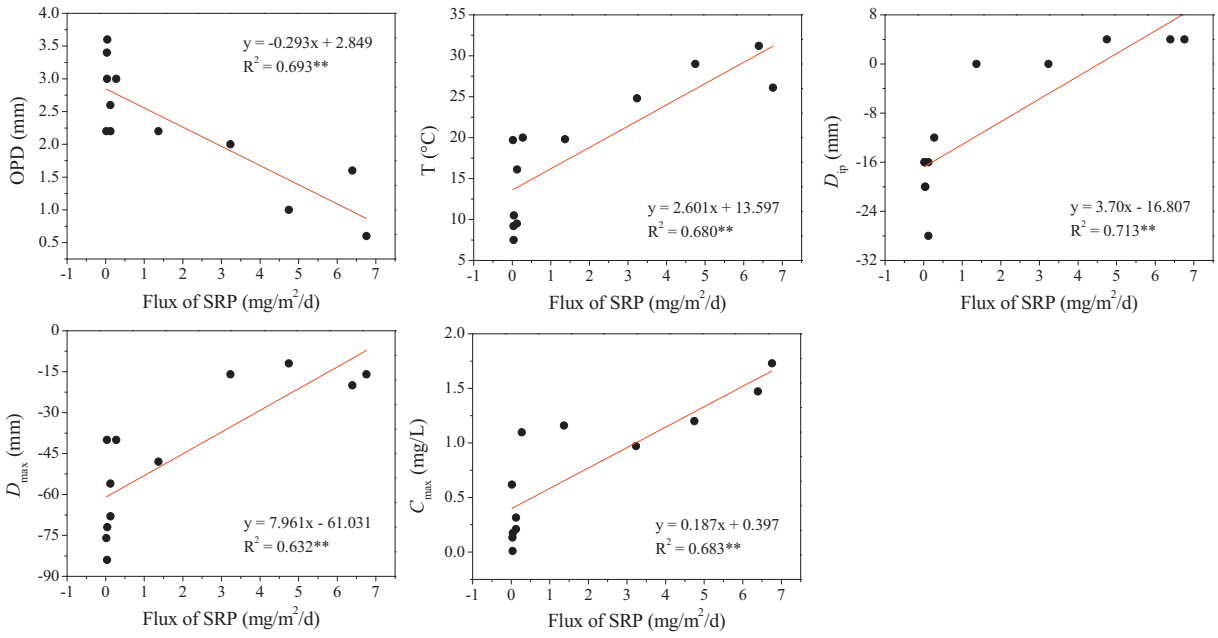

Fig. 8. The SRP flux linear correlations with OPD, temperature and the three profile-featured parameters of mobile P (D_{ip}, D_{max} and C_{max}), between Feb 2016 and Jan 2017.

much greater thickness than previously reported (Giles et al. 2016; Smith et al. 2011).

Iron redox cycling is recognized as a primary factor in the control of P mobility in sediments (Sondergaard et al. 2003). The findings of this study clearly illustrated significant correlations between SRP and soluble Fe(II), reactive Fe and reactive P, and between OPD and SRP flux at the SWI (Figs. 2, 5, 8). On-site, direct evidence was acquired by using simultaneous measurement of labile Fe and P via DGT analysis, showing that DGT-labile P was positively correlated with DGT-labile Fe in 14 sites across Lake Taihu (Ding et al. 2016a). In contrast to the pore water measurements, the DGT measurements reflected the release of Fe(II) and P via reductive dissolution of readily reducible Fe oxyhydroxide (Ding et al. 2016a). This phenomenon has also been observed in other lakes (Gao et al. 2016; Yao et al. 2016). This study therefore provides direct evidence verifying that the seasonal change in P remobilization from sediments is controlled by Fe redox cycling.

Previous studies have revealed that the chemical reduction of Fe oxyhydroxide takes place generally under Eh < 200 mv (Christophoridis and Fytianos 2006), whereas >300 mv values were detected in the upper 35 mm surface sediment layer in this study (Fig. 4; Table 2). This may reflect that the reduction of Fe oxyhydroxide should be largely microbe-mediated (Melton et al. 2014). Attention should be paid to the extremely low contents of reactive Fe and P observed in sediments from April to June (Table 2), which were consistently followed by sharp increases in pore water SRP and soluble Fe(II) from April (Fig. 5). This may be caused by the promotion of microbial reduction of Fe oxyhydroxide as reflected by the increase in the bacterial abundance in March (Table 2).

4.3. Contribution of internal P to seasonal nutrient limitation

The causal role of internal P loading in seasonal N limitation has been emphasized with the establishment of the dual-nutrient paradigm in freshwater ecosystems. The release of P from sediments has the potential to increase the concentration of TP and decrease the ratio of TN/TP in the water column, especially in scenarios where external P inputs have been significantly reduced (e.g., Lake Taihu). As a result, the limiting status transfers from P limitation to N limitation, with this balance regulating the growth of phytoplankton. Several recent studies have tested this hypothesis via field investigation of water columns and modelling. For example, Nikolai and Dzialowski (2014) observed that the anoxic depth (defined as the water column depth where DO <2 mg/L) in an

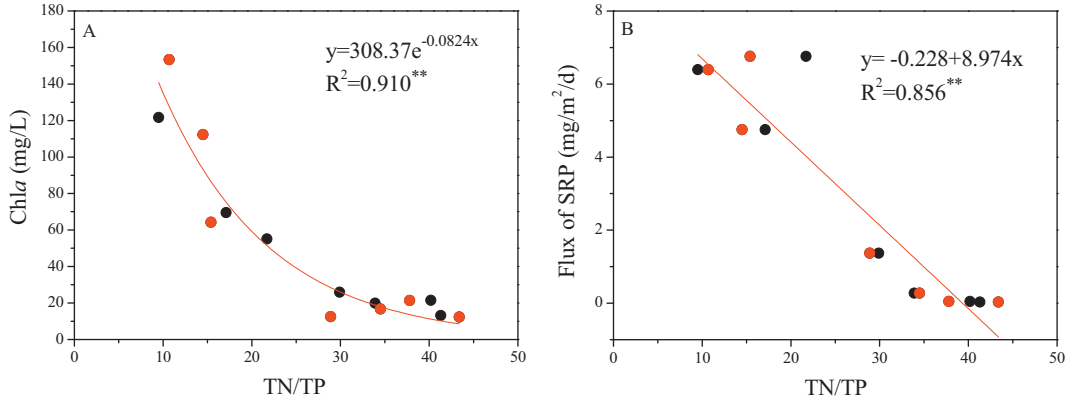

Fig. 9. Relationship between Chl*a* concentration and TN/TP ratio (A) and between SRP flux and TN/TP ratio (B), in Meiliang Bay, Lake Taihu, from February 2015 to January 2017. The red and black dots show the data from February 2015 to January 2016 and from February 2016 to January 2017, respectively.

eutrophic reservoir (Lake Grand, USA) had positive and negative correlations with epilimnetic TP and TN/TP, respectively. Based on these findings, the authors inferred that the internal P load can play an important role in varying nutrient concentrations and TN/TP ratios in the epilimnion of eutrophic reservoirs. Wu et al. (2017) modelled the level of contribution of internal cycling to water eutrophication in a hyper-eutrophic lake (Dianchi, China). Results showed that 77% of TP and 72% of TN total inputs were attributed to the internal loading process, which dictates nutrient limitation in eutrophic lakes.

In this study, the internal load mass of P per unit of sediment area (m^2) was calculated for each month by multiplying the diffusive flux of SRP with the number of days within the month. The total mass of TP in the water column per unit of sediment area (m^2) was also calculated for each month by multiplying the concentration of TP with the total depth of the water column, the results of which are listed in Table 4. The amount of TP in the water column per m^2 increased from 151.2 mg/m^2 in February, to 1242 mg/m^2 in August 2016. The total increase in TP in the water column from February to August (during prebloom-bloom period) was 1091 mg/m^2, while the internal load mass of P ranged from 0.32 mg/m^2 in February to 202.7 mg/m^2 in June. The total released amount of P from February to August was 593.6 mg/m^2, accounting for 54% of the increase in TP observed in the water column during the prebloom-bloom period.

It is of note that the estimation of internal P loading using diffusive flux should be lower than the actual mass, as the release of P from sediments also occurs due to other processes such as hydrodynamic disturbance in shallow lakes. Although this effect was not assessed in this study, Lake Taihu is frequently disturbed by wave processes due to its shallow depth and topography (You et al. 2007). Field observations in Lake Taihu have shown that no significant sediment release of P occurred when wind speeds varied from 0 m/s to 7.0 m/s (Zhu et al. 2007). Conversely, concentrations of SRP in the water column when exposed to a wind rate of 8.0 m/s were twice as high as under no wind conditions (0 m/s), reflecting that strong winds of 8.0 m/s or greater can cause the disturbance and release of P from sediments (Zhu et al. 2005). Yang et al. (2016) further revealed that strong wind-induced increases in nutrients facilitated the growth of cyanobacterial cells to reach a high biomass under relatively low nutrient conditions and it was responsible for 38.3% of the extended bloom events (>300 km^2) from 2007 to 2015 in Lake Taihu.

The present study also investigated the relationship between the diffusive flux of SRP from sediments and TN/TP in the water column, but no correlation was found when analyzing the dataset covering the entire one-year period. However, a significantly negative correlation ($p < 0.01$) was observed between these parameters when comparing data from only the prebloom-bloom period from 2015 to 2016. The underlying assumption was that sediment SRP diffusion fluxes in 2015 were the same as the 2016 values measured for this study (Fig. 9B). This was consistent with the estimation for the contribution of P from internal loading towards TP concentrations in the water column. A recent 3-year monitoring data from TLLER showed that the monthly changes of TP and TN concentrations in the water column of the inner Meiliang Bay were similar to those in the outer bay, while the SRP flux from sediments in the inner bay was greater than that in the outer bay (McCarthy et al. 2007; Zhang et al. 2006). This implies that internal P loading makes a major contribution to the increase in TP concentrations, and therefore, the decrease in TN/TP ratio in the water column of Meiliang Bay during the prebloom-bloom period. The loss of N by denitrification might exacerbate N limitation in Meiliang Bay (McCarthy et al. 2007), although its role should be limited as shown by the relatively small variation in TN concentrations in the water column (Table 1). Further studies are required for combined assessment of the contribution of internal N loading.

Table 4
Mass estimation of the contribution of internal P loading to the monthly change in TP concentrations in the water column, in Meiliang Bay, Lake Taihu, from Feb 2016 to Jan 2017.

Month	TP in the water column (mg/L)	Water depth (m)	Amount of water column P (mg/m^2 sediment)	Cumulative P amount released from sediments (mg/m^2 sediment)
Feb	0.056	2.7	151.2	0.32
Mar	0.078	2.7	210.6	0.94
Arp	0.102	2.7	275.4	8.26
May	0.068	2.8	190.4	42.41
Jun	0.112	3.1	347.2	202.70
Jul	0.233	4.3	1001.9	147.21
Aug	0.462	2.7	1247.4	191.83
Sep	0.221	2.9	640.9	96.97
Oct	0.354	3.3	1168.2	0.12
Nov	0.272	2.8	761.6	2.49
Dec	0.123	2.8	344.4	−0.35
Jan	0.078	2.7	210.6	0.16

4.4. Field implications

The ability of internal P loading to change the nutrient limiting conditions for HABs has been hypothesized, but there has been a lack of direct evidence to support it. This study provides the direct evidence to support that internal P loading can play a causal role in seasonal N limitation in the water column. Furthermore, the vital role of internal P loading occurs during the prebloom-bloom period, when there is a sensitive response by HABs to changes in TN/TP and the transition of nutrient limitation. These results extend the theoretical scope for control of internal P loading through geoenvironmental engineering approaches, such as active capping and stabilization treatments (Mackay et al. 2014), potentially controlling the internal P loading and therefore maintaining P limiting conditions during the prebloom-bloom period. This strategy presents a useful alternative approach to dual nutrient reduction, as P concentrations can be controlled more rapidly and cost-effectively (Douglas et al. 2016).

Acknowledgments

This study was jointly sponsored by the National Natural Science Foundation of China (41621002, 41571465, 41322011), and the National Program for Support of Top-Notch Young Professionals (W02070234). The Taihu Laboratory for Lake Ecosystem Research, Chinese Academy of Sciences (TLLER) provided the environmental monitoring data.

Appendix A. Supplementary data

Supplementary data to this article can be found online at https://doi.org/10.1016/j.scitotenv.2017.12.348.

References

Boudreau, B.P., 1996. The diffusive tortuosity of fine-grained unlithified sediments. Geochim. Cosmochim. Acta 60, 3139–3142.
Brooks, B.W., Lazorchak, J.M., Howard, M.D.A., 2016. Johnson M-VV, Morton SL, Perkins DAK, et al. are harmful algal blooms becoming the greatest inland water quality threat to public health and aquatic ecosystems? Environ. Toxicol. Chem. 35, 6–13.
Bullerjahn, G.S., McKay, R.M., Davis, T.W., Baker, D.B., Boyer, G.L., D'Anglada, L.V., et al., 2016. Global solutions to regional problems: collecting global expertise to address the problem of harmful cyanobacterial blooms. A Lake Erie case study. Harmful Algae 54, 223–238.
Chaffin, J.D., Bridgeman, T.B., Bade, D.L., 2013. Nitrogen constrains the growth of late summer cyanobacterial blooms in Lake Erie. Adv. Microbiol. 3, 16.
Chen, N.W., Peng, B.R., Hong, H.S., Turyaheebwa, N., Cui, S.H., Mo, X.J., 2013. Nutrient enrichment and N:P ratio decline in a coastal bay-river system in southeast China: the need for a dual nutrient (N and P) management strategy. Ocean Coast. Manag. 81, 7–13.
Christophoridis, C., Fytianos, K., 2006. Conditions affecting the release of phosphorus from surface lake sediments. J. Environ. Qual. 35, 1181–1192.
Correll, D.L., 1998. The role of phosphorus in the eutrophication of receiving waters: a review. J. Environ. Qual. 27, 261–266.

Ding, S.M., Sun, Q., Development, Xu D., 2010. Of the DET technique for high-resolution determination of soluble reactive phosphate profiles in sediment pore waters. Int. J. Environ. Anal. Chem. 90, 1130–1138.
Ding, S., Jia, F., Xu, D., Sun, Q., Zhang, L., Fan, C., et al., 2011. High-resolution, two-dimensional measurement of dissolved reactive phosphorus in sediments using the diffusive gradients in thin films technique in combination with a routine procedure. Environ. Sci. Technol. 45, 9680–9686.
Ding, S., Wang, Y., Xu, D., Zhu, C., Zhang, C., 2013. Gel-based coloration technique for the submillimeter-scale imaging of labile phosphorus in sediments and soils with diffusive gradients in thin films. Environ. Sci. Technol. 47, 7821–7829.
Ding, S., Han, C., Wang, Y., Yao, L., Wang, Y., Xu, D., et al., 2015. In situ, high-resolution imaging of labile phosphorus in sediments of a large eutrophic lake. Water Res. 74, 100–109.
Ding, S., Wang, Y., Wang, D., Li, Y.Y., Gong, M., Zhang, C., 2016a. In situ, high-resolution evidence for iron-coupled mobilization of phosphorus in sediments. Sci. Rep. 6, 24341.
Ding, S., Wang, Y., Zhang, L., Xu, L., Gong, M., Zhang, C., 2016b. New holder configurations for use in the diffusive gradients in thin films (DGT) technique. RSC Adv. 6, 88143–88156.
Doig, L.E., North, R.L., Hudson, J.J., Hewlett, C., Lindenschmidt, K.E., Liber, K., 2017. Phosphorus release from sediments in a river-valley reservoir in the northern Great Plains of North America. Hydrobiologia 787, 323–339.
Douglas, G.B., Lurling, M., Spears, B.M., 2016. Assessment of changes in potential nutrient limitation in an impounded river after application of lanthanum-modified bentonite. Water Res. 97, 47–54.
Gao, Y., Liang, T., Tian, S., Wang, L., Holm, P.E., Bruun Hansen, H.C., 2016. High-resolution imaging of labile phosphorus and its relationship with iron redox state in lake sediments. Environ. Pollut. 219, 466–474.
Giles, C.D., Isles, P.D.F., Manley, T., YY, Xu, Druschel, G.K., Schroth, A.W., 2016. The mobility of phosphorus, iron, and manganese through the sediment-water continuum of a shallow eutrophic freshwater lake under stratified and mixed water-column conditions. Biogeochemistry 127, 15–34.
Guildford, S.J., Hecky, R.E., 2000. Total nitrogen, total phosphorus, and nutrient limitation in lakes and oceans: is there a common relationship? Limnol. Oceanogr. 45, 1213–1223.
Ho, J.C., Michalak, A.M., 2017. Phytoplankton blooms in Lake Erie impacted by both long-term and springtime phosphorus loading. J. Great Lakes Res. 43, 221–228.
Janssen, A.B.G., de Jager, V.C.L., Janse, J.H., Kong, X., Liu, S., Ye, Q., et al., 2017. Spatial identification of critical nutrient loads of large shallow lakes: implications for Lake Taihu (China). Water Res. 119, 276–287.
Jeppesen, E., Sondergaard, M., Jensen, J.P., Havens, K.E., Anneville, O., Carvalho, L., et al., 2005. Lake responses to reduced nutrient loading - an analysis of contemporary long-term data from 35 case studies. Freshw. Biol. 50, 1747–1771.
Klausmeier, C.A., Litchman, E., Daufresne, T., Levin, S.A., 2004. Optimal nitrogen-to-phosphorus stoichiometry of phytoplankton. Nature 429, 171–174.
Lepori, F., Roberts, J.J., 2017. Effects of internal phosphorus loadings and food-web structure on the recovery of a deep lake from eutrophication. J. Great Lakes Res. 43, 255–264.
Lewis, W.M., Wurtsbaugh, W.A., 2008. Control of lacustrine phytoplankton by nutrients: erosion of the phosphorus paradigm. Int. Rev. Hydrobiol. 93, 446–465.
Lewis, W.M., Wurtsbaugh, W.A., Paerl, H.W., 2011. Rationale for control of anthropogenic nitrogen and phosphorus to reduce eutrophication of inland waters. Environ. Sci. Technol. 45, 10300–10305.
Ma, J.R., Qin, B.Q., Wu, P., Zhou, J., Niu, C., Deng, J.M., et al., 2015. Controlling cyanobacterial blooms by managing nutrient ratio and limitation in a large hyper-eutrophic lake: lake Taihu, China. J. Environ. Sci. 27, 80–86.
Mackay, E.B., Maberly, S.C., Pan, G., Reitzel, K., Bruere, A., Corker, N., et al., 2014. Geoengineering in lakes: welcome attraction or fatal distraction? Inland Waters 4, 349–356.
Matisoff, G., Kaltenberg, E.M., Steely, R.L., Hummel, S.K., Seo, J., Gibbons, K.J., et al., 2016. Internal loading of phosphorus in western Lake Erie. J. Great Lakes Res. 42, 775–788.
McCarthy, M.J., Lavrentyev, P.J., Yang, L., Zhang, L., Chen, Y., Qin, B., et al., 2007. Nitrogen dynamics and microbial food web structure during a summer cyanobacterial bloom in a subtropical, shallow, well-mixed, eutrophic lake (lake Taihu, China). Hydrobiologia 581, 195–207.
Melton, E.D., Swanner, E.D., Behrens, S., Schmidt, C., Kappler, A., 2014. The interplay of microbially mediated and abiotic reactions in the biogeochemical Fe cycle. Nat. Rev. Microbiol. 12, 797–808.
Nikolai, S.J., Dzialowski, A.R., 2014. Effects of internal phosphorus loading on nutrient limitation in a eutrophic reservoir. Limnol. – Ecol. Manag. Inland Waters 49, 33–41.
Nürnberg, G.K., LaZerte, B.D., 2016. More than 20 years of estimated internal phosphorus loading in polymictic, eutrophic Lake Winnipeg, Manitoba. J. Great Lakes Res. 42, 18–27.
Nürnberg, G.K., LaZerte, B.D., Loh, P.S., Molot, L.A., 2013. Quantification of internal phosphorus load in large, partially polymictic and mesotrophic Lake Simcoe, Ontario. J. Great Lakes Res. 39, 271–279.
Orihel, D.M., Schindler, D.W., Ballard, N.C., Graham, M.D., O'Connell, D.W., Wilson, L.R., et al., 2015. The "nutrient pump:" iron-poor sediments fuel low nitrogen-to-phosphorus ratios and cyanobacterial blooms in polymictic lakes. Limnol. Oceanogr. 60, 856–871.
Otten, T.G., Xu, H., Qin, B., Zhu, G., Paerl, H.W., 2012. Spatiotemporal patterns and ecophysiology of toxigenic Microcystis blooms in Lake Taihu, China: implications for water quality management. Environ. Sci. Technol. 46, 3480–3488.
Paerl, H.W., Otten, T.G., 2013. Harmful cyanobacterial blooms: causes, consequences, and controls. Microb. Ecol. 65, 995–1010.
Paerl, H.W., Scott, J.T., McCarthy, M.J., Newell, S.E., Gardner, W.S., Havens, K.E., et al., 2016. It takes two to tango: when and where dual nutrient (N & P) reductions are needed to Protect Lakes and downstream ecosystems. Environ. Sci. Technol. 50, 10805–10813.
Paytan, A., Roberts, K., Watson, S., Peek, S., Chuang, P.-C., Defforey, D., et al., 2017. Internal loading of phosphate in Lake Erie Central Basin. Sci. Total Environ. 579, 1356–1365.
Penn, M.R., Auer, M.T., Doerr, S.M., Driscoll, C.T., Brooks, C.M., Effler, S.W., 2000. Seasonality in phosphorus release rates from the sediments of a hypereutrophic lake under a matrix of pH and redox conditions. Can. J. Fish. Aquat. Sci. 57, 1033–1041.
Peñuelas, J., Poulter, B., Sardans, J., Ciais, P., van der Velde, M., Bopp, L., et al., 2013. Human-induced nitrogen–phosphorus imbalances alter natural and managed ecosystems across the globe. Nat. Commun. 4, 2934.
Qin, B., Hu, W., Chen, W., 2004. Process and Mechanism of Environmental Changes of the Taihu Lake. Book in Chinese. Science Press, Beijing.
Qin, B., Zhu, G., Gao, G., Zhang, Y., Li, W., Paerl, H.W., et al., 2010. A drinking water crisis in Lake Taihu, China: linkage to climatic variability and Lake management. Environ. Manag. 45, 105–112.
Santner, J., Larsen, M., Kreuzeder, A., Glud, R.N., 2015. Two decades of chemical imaging of solutes in sediments and soils – a review. Anal. Chim. Acta 878, 9–42.
Schelske, C.L., 2009. Eutrophication: focus on phosphorus. Science 324, 722.
Schindler, D.W., Hecky, R.E., Findlay, D.L., Stainton, M.P., Parker, B.R., Paterson, M.J., et al., 2008. Eutrophication of lakes cannot be controlled by reducing nitrogen input: results of a 37-year whole-ecosystem experiment. Proc. Natl. Acad. Sci. U. S. A. 105, 11254–11258.
Schindler, D.W., Carpenter, S.R., Chapra, S.C., Hecky, R.E., Orihel, D.M., 2016. Reducing phosphorus to curb Lake eutrophication is a success. Environ. Sci. Technol. 50, 8923–8929.
Smith, V.H., 2006. Responses of estuarine and coastal marine phytoplankton to nitrogen and phosphorus enrichment. Limnol. Oceanogr. 51, 377–384.
Smith, L., Watzin, M.C., Druschel, G., 2011. Relating sediment phosphorus mobility to seasonal and diel redox fluctuations at the sediment-water interface in a eutrophic freshwater lake. Limnol. Oceanogr. 56, 2251–2264.
Sondergaard, M., Jensen, J.P., Jeppesen, E., 2003. Role of sediment and internal loading of phosphorus in shallow lakes. Hydrobiologia 506, 135–145.
Søndergaard, M., Bjerring, R., Jeppesen, E., 2013. Persistent internal phosphorus loading during summer in shallow eutrophic lakes. Hydrobiologia 710, 95–107.
Spears, B.M., Carvalho, L., Perkins, R., Kirika, A., Paterson, D.M., 2012. Long-term variation and regulation of internal phosphorus loading in loch Leven. Hydrobiologia 681, 23–33.
Tong, Y., Zhang, W., Wang, X., Couture, R.-M., Larssen, T., Zhao, Y., et al., 2017. Decline in Chinese lake phosphorus concentration accompanied by shift in sources since 2006. Nat. Geosci. 10, 507–511.
Verburg, P., Horrox, J., Chaney, E., Rutherford, J.C., Quinn, J.M., Wilcock, R.J., et al., 2013. Nutrient ratios, differential retention, and the effect on nutrient limitation in a deep oligotrophic lake. Hydrobiologia 718, 119–130.
Watson, S.B., Miller, C.J., Arhonditsis, G.B., Boyer, G.L., Carmichael, W.W., Charlton, M.N., et al., 2016. The re-eutrophication of Lake Erie: harmful algal blooms and hypoxia. Harmful Algae 56, 44–66.
Welch, E.B., Cooke, G.D., 2005. Internal phosphorus loading in shallow lakes: importance and control. Lake Reservoir Manage. 21, 209–217.
Wu, H., Hu, Y., 2008. Maintaining healthy rivers and lakes through water diversion from Yangtze River to Taihu Lake in Taihu Basin. Water Sci. Eng. 1, 36–43.
Wu, Z., Liu, Y., Liang, Z., Wu, S., Guo, H., 2017. Internal cycling, not external loading, decides the nutrient limitation in eutrophic lake: a dynamic model with temporal Bayesian hierarchical inference. Water Res. 116, 231–240.
Xie, L.Q., Xie, P., Tang, H.J., 2003. Enhancement of dissolved phosphorus release from sediment to lake water by Microcystis blooms-an enclosure experiment in a hyper-eutrophic, subtropical Chinese lake. Environ. Pollut. 122, 391–399.
Xu, D., Wu, W., Ding, S., Sun, Q., Zhang, C., 2012. A high-resolution dialysis technique for rapid determination of dissolved reactive phosphate and ferrous iron in pore water of sediments. Sci. Total Environ. 421–422, 245–252.
Xu, H., Paerl, H., Qin, B., Zhu, G., Hall, N., Wu, Y., 2014. Determining critical nutrient thresholds needed to control harmful cyanobacterial blooms in eutrophic Lake Taihu, China. Environ. Sci. Technol. 49, 1051–1059.
Xu, H., Paerl, H.W., Qin, B., Zhu, G., Hall, N.S., Wu, Y., 2015. Determining critical nutrient thresholds needed to control harmful cyanobacterial blooms in eutrophic Lake Taihu, China. Environ. Sci. Technol. 49, 1051–1059.
Xu, H., Paerl, H.W., Zhu, G., Qin, B., Hall, N.S., Zhu, M., 2017. Long-term nutrient trends and harmful cyanobacterial bloom potential in hypertrophic Lake Taihu, China. Hydrobiologia 787, 229–242.
Yang, S.-Q., Liu, P.-W., 2010. Strategy of water pollution prevention in Taihu Lake and its effects analysis. J. Great Lakes Res. 36, 150–158.
Yang, L., Lei, K., Yan, W., Li, Y., 2013. Internal loads of nutrients in Lake Chaohu of China: implications for lake eutrophication. Int. J. Environ. Res. Public Health 7, 1021–1028.
Yang, Z., Zhang, M., Shi, X., Kong, F., Ma, R., Nutrient, Yu Y., 2016. Reduction magnifies the impact of extreme weather on cyanobacterial bloom formation in large shallow Lake Taihu (China). Water Res. 103, 302–310.
Yao, Y., Wang, P., Wang, C., Hou, J., Miao, L., Yuan, Y., et al., 2016. Assessment of mobilization of labile phosphorus and iron across sediment-water interface in a shallow lake (Hongze) based on in situ high-resolution measurement. Environ. Pollut. 219, 873–882.
You, B.S., Zhong, J.C., Fan, C.X., Wang, T.C., Zhang, L., Ding, S.M., 2007. Effects of hydrodynamics processes on phosphorus fluxes from sediment in large, shallow Taihu Lake. J. Environ. Sci. 19, 1055–1060.
Zhang, H., Davison, W., 1995. Performance characteristics of diffusion gradients in thin films for the in situ measurement of trace metals in aqueous solution. Anal. Chem. 67, 3391–3400.

Zhang, L., Fan, C.X., Wang, J.J., Zheng, C.H., 2006. Space-time dependent variances of ammonia and phosphorus flux on sediment-water Interface in Lake Taihu environmental. Science 27, 1537–1543.
Zhang, C., Ding, S., Xu, D., Tang, Y., Wong, M., 2014. Bioavailability assessment of phosphorus and metals in soils and sediments: a review of diffusive gradients in thin films (DGT). Environ. Monit. Assess. 186, 7367–7378.
Zhu, G., Qin, B., Gao, G., 2005. Direct evidence of phosphorus outbreak release from sediment to overlying water in a large shallow lake caused by strong wind wave disturbance. Chin. Sci. Bull. 50, 577–582.
Zhu, G., Qin, B., Gao, G., Zhang, L., Luo, L., Zhang, Y., 2007. Effects of hydrodynamics on phosphorus concentrations in water of Lake Taihu, a large, shallow, eutrophic lake of China. Hydrobiologia 581, 53–61.